Original paper

Babánekite, $Cu_3(AsO_4)_2 \cdot 8H_2O$, from Jáchymov, Czech Republic – a new member of the vivianite group

Jakub PLÁŠIL[1*], Pavel ŠKÁCHA[2, 3], Jiří SEJKORA[2], Radek ŠKODA[4], Milan NOVÁK[4], František VESELOVSKÝ[5], Jan HLOUŠEK[†]

[1] *Institute of Physics, Academy of Sciences of the Czech Republic (ASCR) v.v.i, Na Slovance 2, 182 21 Prague 8, Czech Republic; plasil@fzu.cz*
[2] *Department of Mineralogy and Petrology, National Museum, Cirkusová 1740, 193 00 Prague 9, Czech Republic*
[3] *Mining Museum Příbram, Hynka Kličky Place 293, 261 01 Příbram VI – Březové Hory, Czech Republic*
[4] *Department of Geological Sciences, Faculty of Science, Masaryk University, Kotlářská 2, 611 37 Brno, Czech Republic*
[5] *Czech Geological Survey, Geologická 6, 152 00 Prague 5, Czech Republic*
[†] *Jáchymov; deceased on April 27, 2014*
[*] *Corresponding author*

Babánekite, $Cu_3(AsO_4)_2 \cdot 8H_2O$, a new member of the vivianite group was found in material originating from the Geister vein, Rovnost mine, Jáchymov, Western Bohemia, Czech Republic. It occurs as a supergene alteration mineral in association with members of the lindackerite supergroup (veselovskýite, hloušekite, pradetite and lindackerite), lavendulan, gypsum and an X-ray amorphous Cu–Al–Si–O–H phase. Crystals of babánekite are pinkish to peach-colored, elongated, prismatic and up to 2 mm in length. They exhibit the forms {010}, {100}, {110}, {101} and less frequently also {001}. Crystals are transparent to translucent with a vitreous luster. The mineral has a light pinkish streak. Estimated Mohs hardness is between 1.5 and 2. The cleavage is perfect on {010}. The calculated density is 3.192 g/cm^3. Electron-microprobe analysis yielded CoO 8.89, NiO 4.06, CuO 15.31, ZnO 10.87, P_2O_5 0.16, As_2O_5 39.79, SO_3 0.13, H_2O 24.78 (calc.), total 103.99 wt.% giving the empirical formula $(Cu_{1.12}Zn_{0.78}Co_{0.69}Ni_{0.32})_{\Sigma 2.91}[(AsO_4)_{2.01}(PO_4)_{0.01}(SO_4)_{0.01}]_{\Sigma 2.03} \cdot 8H_2O$ based on 16 O *apfu*. The ideal end-member formula of babánekite is $Cu_3(AsO_4)_2 \cdot 8H_2O$, which requires CuO 38.95, As_2O_5 37.52, H_2O 23.53, total 100.00 wt.%. Babánekite is monoclinic, *C*2/*m*, with a = 10.1729(3), b = 13.5088(4), c = 4.7496(1) Å, β = 105.399(2)°, V = 629.28(3) Å^3 and Z = 2. The eight strongest X-ray powder diffraction lines are [d_{obs} Å(I)(*hkl*)]: 7.936(11)(110), 6.743(100)(020), 3.231(14)(13-1), 2.715(11)(041), 2.3331(10)(15-1), 2.0819(5)(350), 1.6862(16)(080) and 1.6107(4)(55-1). The crystal structure of babánekite, refined to R_1 = 2.18 % for 864 unique observed reflections, confirmed that the atomic arrangement is similar to other members of the vivianite group of minerals. The mineral is named for Ing. František Babánek (1836–1910), Czech mining and geological expert, who worked in the Jáchymov and Příbram mines.

Keywords: babánekite, new mineral, vivianite group, crystal structure, Jáchymov
Received: 13 September, 2017; accepted: 3 January, 2018; handling editor: F. Laufek
The online version of this article (doi: 10.3190/jgeosci.248) contains supplementary electronic material.

1. Introduction

The vivianite group unifies hydrated arsenates and phosphates with the generalized structural formula $Me_3(XO_4)_2(H_2O)_8$, where *Me* designates sites that are occupied by various divalent cations and *X* the site occupied by As^{5+} or P^{5+}. To date, six As-dominant members of this group are known: annabergite (Ni), erythrite (Co), hörnesite (Mg), manganohörnesite (Mn), köttigite (Zn) and parasymplesite (Fe). In addition, four P-dominant members have been described: arupite (Ni), barićite (Mg, Fe), pakhomovskyite (Co) and vivianite (Fe). Broad solid-solutions taking place at the cationic sites have been established especially for As-dominant members.

In this work we report on the new mineral species babánekite, ideally $Cu_3(AsO_4)_2 \cdot 8H_2O$. It is a Cu- and As-dominant member of the vivianite group that was found in the Rovnost mine, Jáchymov, Czech Republic. The new mineral honors the Senior Mining Counselor ("Oberbergrath") František Babánek (born October 10, 1836, in Kamenný Přívoz near Jílové, Bohemia; died February 25, 1910, in Prague). František Babánek was a Czech mining expert, geologist and mineralogist. During his active service, he worked in Příbram and later in Jáchymov, the two most important mining districts in Bohemia, then a part of the Austro-Hungarian Empire.

The new mineral was approved by the CNMNC IMA under the code IMA 2012-007. The type specimen is deposited in the collections of the Department of Mineralogy and Petrology of the National Museum, Prague, Czech Republic, catalog number: P1P 8/2011.

2. Occurrence

The Jáchymov ore district (Western Bohemia, Krušné hory Mountains, Czech Republic) presents a classic example of Ag–As–Bi–Co–Ni–U hydrothermal vein-type mineralization (Ondruš et al. 2003; Hloušek et al. 2014). The ore-bearing veins cut medium-grade metasedimentary rocks of Cambrian to Ordovician age, which surround a Variscan granitic pluton. The majority of the primary ore minerals were deposited from mesothermal fluids during Variscan mineralizing processes. More than 430 minerals have been described from Jáchymov, including an extremely diverse assemblage of supergene minerals (see Ondruš et al. 1997, 2003; Hloušek et al. 2014 for review).

Babánekite was found in an old ore-stope on the Geister vein at the 3rd Geister level of the Rovnost (former Werner) mine. The particular locality, Geister vein, was opened by old mining workings from the surface down to the level of the Daniel drainage adit, at the 1st, 3rd, 6th, Barbora and Daniel levels. This vertical sequence mostly represents a supergene oxidation zone of the vein opened by mining workings, with the very rich zones of the supergene cementation Ag–Hg mineralization at the two last mentioned adit levels (Vogl 1854; Škácha et al. 2014).

The old, near-surface workings (from the 1st to the 6th level), originating partly from the 16th century, were re-opened during the first half of the 19th century. The main aim was mining for U, used for glass-staining, and later mostly for extraction of radium. The re-opening of the 3rd and 6th Geister levels was well documented by the mining official Josef Florian Vogl, after whom the mineral voglite is named (Haidinger 1853; Ondruš et al. 1997). Vogl (1856a, b) described in detail a varied supergene mineral association from the Geister vein constituted by arsenates of the vivianite group and lindackerite supergroup, as well as supergene uranyl-bearing minerals. The richness of the locality results from the occurrence of both the recently/sub-recently formed minerals connected with the post-mining processes and the supergene minerals formed *in-situ* in the oxidation zone (association of uranyl arsenates and vanadates; association of Pb–Cu supergene minerals and minerals containing Y + *REE*).

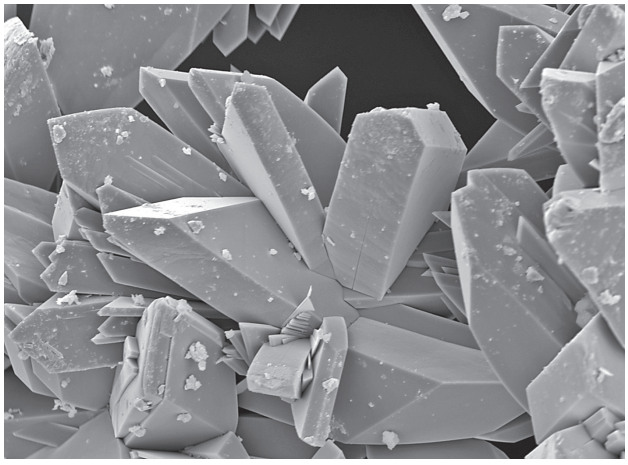

Fig. 1 Detail of babánekite crystals. Secondary electron (SE) image (Hitachi 3700N), 150 μm wide.

Babánekite was found by one of the authors (PŠ) in an old mining field informally called the "lindackerite stope" by mineral collectors. The name is due to frequent occurrences of the lindackerite-supergroup minerals: lindackerite, veselovskýite (Sejkora et al. 2010), hloušekite (Plášil et al. 2014a), pradetite (unpublished data of the authors) and klajite (Plášil et al. 2014b; Hloušek et al. 2014). These minerals crystallize on the strongly altered ore-body consisting mainly of massive tennantite, galena and chalcopyrite with disseminated uraninite in quartz. Babánekite aggregates grow in cavities and on the surface of ore fragments. In close association with babánekite, members of the lindackerite supergroup, lavendulan, gypsum and X-ray amorphous Cu–Al–Si–O–H material were detected, overgrowing relics of the primary minerals partly cemented by supergene mineralization.

3. Physical and optical properties

Babánekite forms elongated, prismatic crystals (Fig. 1) up to 1.5 mm in length, grouped in hemispherical aggregates up to 2 mm (Fig. 2). Crystals exhibit the forms {010}, {100}, {110}, {101} and less frequently also {001}. Crystals, transparent to translucent, are pinkish to peach in color and have a vitreous luster. Babánekite has a light pink streak. The Mohs hardness is estimated between 1.5 and 2.5 (in analogy with other As-dominant members of the vivianite group). Prismatic crystals show perfect cleavage on {010}. A density of 3.192 g/cm^3 was calculated using the empirical formula and unit-cell parameters obtained from single-crystal X-ray diffraction. Direct density measurements were not undertaken due to paucity of pure material. Babánekite is non-fluorescent under short- or long-wave UV radiation. Optical properties could not be determined due to zonation of the babánekite crystals available (Fig. 3); the calculated (Gladstone–Dale rule) average n is 1.6615.

4. Chemical composition

The chemical composition of babánekite was determined at Masaryk University in Brno using a Cameca SX100 electron microprobe (WDS mode, 15 kV, 5 nA, and 10 μm beam diameter). The following X-ray lines and standards were selected: K_α lines: P (fluorapatite), Zn (ZnO), Cu (lammerite), Co (metallic Co), Ni (Ni) and S (baryte),

Fig. 2 Babánekite crystal aggregates consisting of elongated prismatic crystals of dominating {010} faces. The bluish material is a PXRD-amorphous Cu–Al–Si–O–H phase; metallic minerals are tennantite and chalcopyrite. The width of the image is 3.5 mm.

L_α line: As (lammerite). Other elements, including Al, Bi, Ca, Cl, Fe, K, Mg, Mn, Na, Pb, Si and V, were also sought, but not found (the detection limits for these elements are ~0.05–0.10 wt.% at the analytical conditions used). Peak counting times were 10–20 s and the counting time for the background their half. The measured intensities were processed for matrix effects using the "*PAP*" correction routine (Pouchou and Pichoir 1985). The H_2O content (8 *pfu*) was calculated based on the stoichiometry obtained from the structure data and by analogy with other vivianite-group minerals.

An aggregate removed from the holotype specimen – that was also used for single-crystal and powder X-ray diffraction experiments – is characterized by the presence of slightly Cu^{2+}-dominated crystals (0.80–1.47 *apfu* Cu) with sectors/zones enriched by Zn^{2+} (up to 1.03) or Co^{2+} (up to 0.84) or Ni^{2+} (up to 0.50 *apfu*) (Fig. 3). In any case, Cu^{2+} is significantly prevailing in all zones (Fig. 4). The results of electron microprobe analyses of this aggregate (11 point analyses) are summarized in Tab. 1.

Tab. 1 Chemical composition of babánekite from Jáchymov

Constituent	Mean of 11 spots (wt. %)	Range	SD
CoO	8.89	6.48–10.65	0.04
NiO	4.06	1.20–6.26	0.09
CuO	15.31	10.72–20.01	3.47
ZnO	10.87	8.70–14.51	2.20
P_2O_5	0.16	0.10–0.24	0.04
As_2O_5	39.79	39.01–40.58	0.57
SO_3	0.13	0.00–0.37	0.11
H_2O*	24.78		
Total	103.99		

* H_2O content was calculated from stoichiometry (8 H_2O) derived from the crystal-structure study
SD – standard deviation

The empirical formula of babánekite (calculated on the basis of 16 O *apfu*) is $(Cu_{1.12}Zn_{0.78}Co_{0.69}Ni_{0.32})_{\Sigma 2.91}[(AsO_4)_{2.01}(PO_4)_{0.01}(SO_4)_{0.01}]_{\Sigma 2.03} \cdot 8H_2O$. This formula shows a certain Me^{2+}-deficiency and thus it is not fully charge balanced (having 0.26 of negative charge excess). The possible presence of other cations (Ca, Pb, Fe, Mg, Mn...) in concentrations under detection limits of the measurement is then the most suitable explanation. The results of crystal structure study do not indicate a presence of OH groups in this mineral. The ideal end-member formula of babánekite is $Cu_3(AsO_4)_2 \cdot 8H_2O$, which requires CuO 38.95, As_2O_5 37.52 and H_2O 23.53, total 100.00 wt. %.

Subsequently, we also determined the chemical composition of other crystal aggregates from the holotype sample and also from four additional samples of babánekite from the same locality (Geister vein, Jáchy-

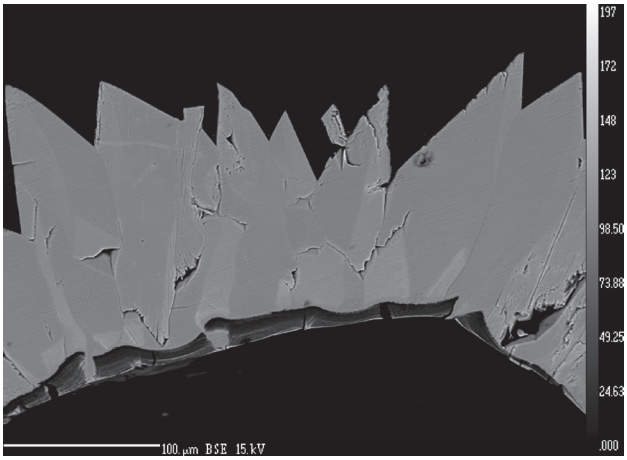

Fig. 3 Zonation of babánekite crystals mainly due to variable Zn contents. Back-scattered electron (BSE) image (Cameca SX100).

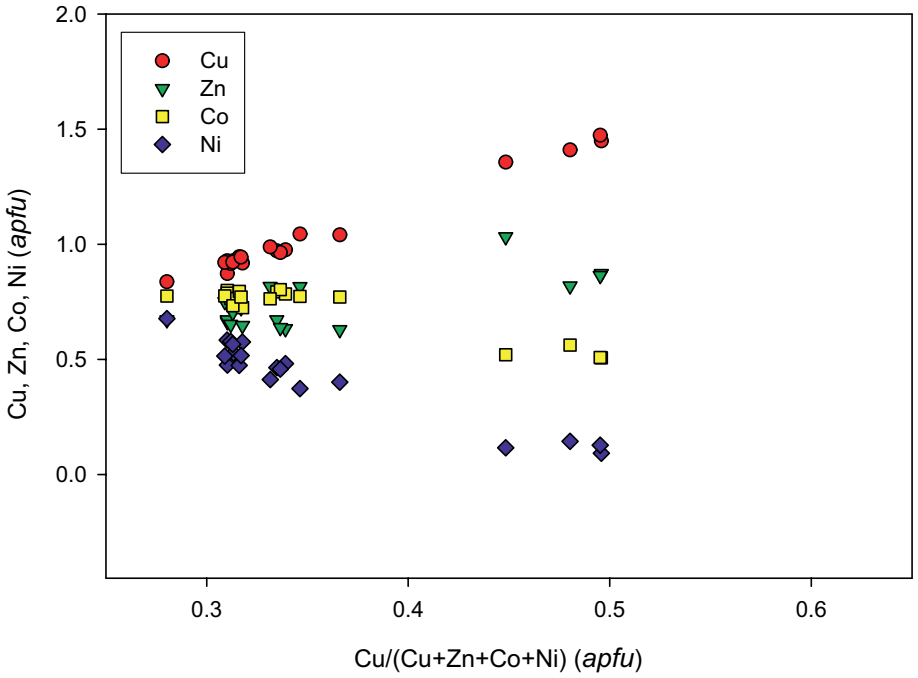

Fig. 4 Plot of Cu/(Cu + Zn + Co + Ni) *vs.* individual contents of Cu, Zn, Co and Ni (all in *apfu*) for the holotype sample of babánekite from Jáchymov.

mov), preserved mostly in collections of private mineral collectors. Additional analyses of crystals removed later from the holotype specimen resemble original analyses used for the mineral proposal for CNMNC of IMA (Fig. 4). Apparently, the Cu^{2+} content correlates negatively both with Ni^{2+} and Co^{2+}, but not with Zn^{2+}. Other samples of babánekite from Geister vein investigated by EMPA differ significantly particularly in the Zn^{2+} contents (Fig. 5), which do not exceed 0.14 Zn *apfu*, along with the even more dominating Cu^{2+} than for holotype specimen, reaching up to 1.78 Cu *pfu*. The Cu^{2+} contents again correlate negatively with Ni^{2+} (or Ni + Co).

5. X-ray crystallography and crystal structure

The X-ray powder diffraction pattern of babánekite (Tab. 2) was obtained from a hand-picked sample utilizing a Bruker D8 Advance diffractometer (National Museum, Prague) with a solid-state 1D LynxEye detector using CuK_α radiation (40 kV, 40 mA). For minimizing the background of the scan, the powder sample was placed onto the surface of a flat silicon wafer from acetone suspension. Powder data were collected in the Bragg–Brentano geometry covering the range 5–70° 2θ, with the step size of 0.01° and counting time of 30 s per step (total time of experiment about three days). Positions and intensities of diffraction maxima were found and refined using the Pear-

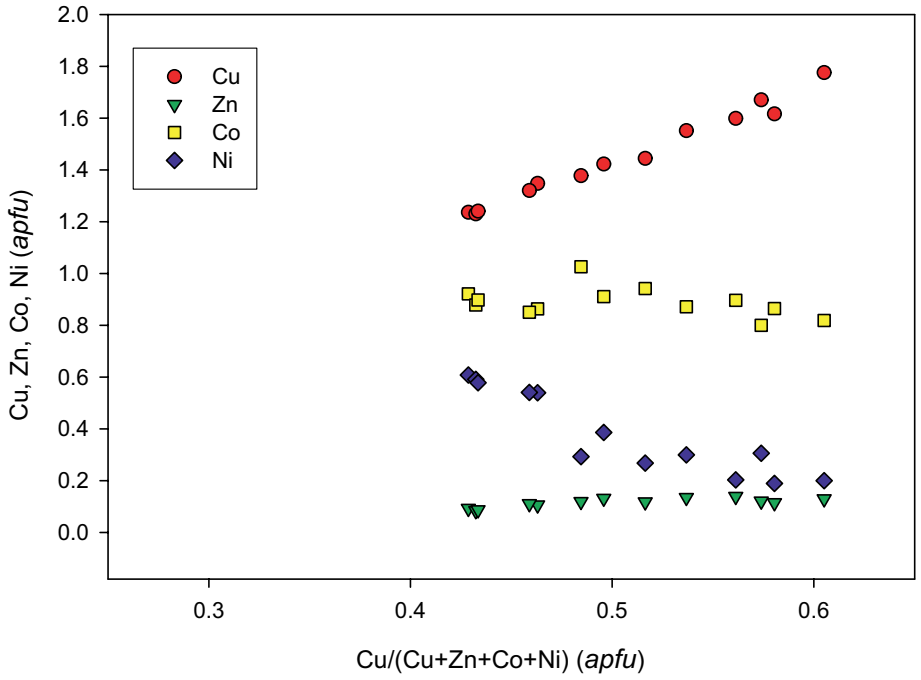

Fig. 5 Plot of Cu/(Cu + Zn + Co + Ni) *vs.* individual contents of Cu, Zn, Co and Ni (all in *apfu*) for other studied samples of babánekite from the Geister vein, Jáchymov.

sonVII profile-shape function of the ZDS program package (Ondruš 1995), and the unit-cell parameters were refined by the least-squares algorithm implemented by Burnham (1962).

Refined unit-cell parameters are a = 10.1850(6), b = 13.4852(6), c = 4.7484(3) Å, β = 105.316(5)°, with V = 629.01(6) Å^3. Some observed differences (in the range 0.001–0.02 Å) between parameters obtained from powder and single-crystal data are probably caused by the slightly different chemical composition of the samples (i.e., zonation; see Figs 3 and 4) by these studies.

A 0.097 × 0.037 × 0.034 mm prismatic crystal of babánekite was selected for single-crystal X-ray diffraction experiment using an Oxford diffraction Gemini single-crystal four-circle diffractometer. Graphite-monochromatized MoK_α radiation (λ = 0.71073 Å) from a conventional sealed X-ray tube was collimated with a fiber-optics Mo-Enhance collimator and detected with an Atlas CCD detector. The unit cell of babánekite was refined from 3645 reflections by the least-squares algorithm of the Crysalis-Pro package giving a monoclinic cell with: a = 10.1742(2), b = 13.5104(3), c = 4.7489(1) Å, β = 105.416(2)° and V = 629.29(3) Å^3, Z = 2. From the total of 5722 measured reflections, 1005 were unique, and 864 were classified as unique observed with the criterion [$I_{obs} > 3\sigma(I)$]. An empirical (multi-scan) correction for absorption was applied. The summary of data collection, crystallographic data and refinement are listed in Tab. 3.

The crystal structure of babánekite was refined from the single-crystal X-ray data using the known structure model for erythrite (Wildner et al. 1996) and the full-matrix least-squares algorithm of the Jana2006 software (Petříček et al. 2014) based on F^2. All non-H atoms were refined anisotropically. In the last cycles of the refinement, the occupancies of the Cu sites were also refined. The refined site occupancy of the Cu sites, giving a sum of 2.92 atoms per unit cell, suggests that Cu is mixed at the sites with lighter atoms such as Co or Ni and also heavier, as Zn, as well.

Tab. 2 Powder X-ray diffraction data for babánekite

I_{rel}	d_{obs}	d_{calc}	I_{calc}	h	k	ℓ	I_{rel}	d_{obs}	d_{calc}	I_{calc}	h	k	ℓ
11	7.936	7.940	37	1	1	0	3	2.1965	2.1966	4	1	5	1
100	6.743	6.743	100	0	2	0	3	2.1965	2.1969	6	2	2	–2
2	4.909	4.912	10	2	0	0	5	2.0819	2.0818	12	3	5	0
1	4.581	4.580	5	0	0	1	1	2.0437	2.0437	1	2	6	0
3	4.394	4.394	15	1	1	–1	1	2.0171	2.0177	2	0	6	1
4	4.087	4.087	5	1	3	0	1	1.9822	1.9822	3	4	4	–1
1	3.969	3.970	2	2	2	0	1	1.9503	1.9499	5	3	3	–2
2	3.903	3.903	14	2	0	–1	1	1.9443	1.9441	4	5	1	0
1	3.644	3.645	8	1	1	1	2	1.9105	1.9102	11	1	3	2
4	3.370	3.371	2	0	4	0	1	1.8331	1.8333	3	5	3	–1
14	3.231	3.231	41	1	3	–1	<1	1.7942	1.7944	1	2	6	1
2	3.181	3.182	8	3	1	0	1	1.7854	1.7856	2	3	5	1
5	2.999	2.999	19	3	1	–1	2	1.7795	1.7796	3	1	7	–1
5	2.980	2.980	26	2	0	1	16	1.6862	1.6856	8	0	8	0
4	2.779	2.780	7	2	4	0	3	1.6618	1.6620	10	1	5	2
5	2.725	2.726	24	2	2	1	4	1.6107	1.6106	4	5	5	–1
11	2.715	2.715	19	0	4	1	1	1.5909	1.5910	3	6	2	0
5	2.646	2.647	17	3	3	0	1	1.5524	1.5524	4	5	3	1
1	2.601	2.601	1	1	5	0	<1	1.5376	1.5378	4	6	0	–2
3	2.551	2.551	6	2	4	–1	1	1.5105	1.5105	4	6	4	–1
3	2.4510	2.4506	17	4	0	–1	2	1.4900	1.4899	5	4	0	2
10	2.3331	2.3327	17	1	5	–1	2	1.4672	1.4672	5	2	8	1
1	2.3040	2.3032	7	4	2	–1	1	1.4103	1.4101	3	5	5	1
2	2.2474	2.2475	1	0	6	0	2	1.3888	1.3888	3	4	8	–1
1	2.2325	2.2327	2	2	4	1							

d values quoted in Å

Tab. 3 Crystallographic data and refinement details for babánekite

Structural formula	$Cu_3(AsO_4)_2(H_2O)_8$
a, b, c [Å]	10.1729(3), 13.5088(4), 4.7496(1)
β [°]	105.399(2)
V [Å^3]	629.28(3)
Z	2
D_{calc} [g/cm^3]	3.206
Space group	*C*2/*m*
Temperature	298 K
Detector; wavelength	Atlas CCD; MoK_α (0.71073 Å)
Crystal dimensions [mm]	0.097 × 0.037 × 0.034
Collection mode	ω rotational scans
Limiting θ angles [°]	3.02–31.13°
Limiting Miller indices	–13<*h*<14, –18<*k*<19, –6<*l*<6
No. of reflections	5722
No. of unique reflections	1005
No. of observed reflections (criterion)	864 [I_{obs}>3σ(*I*)]
R_{int}, coverage	0.033, 95%
Absorption correction (mm^{-1}), method	10.20, multi-scan
Transmission (min/,max)	0.514/0.730
F_{000}	589
Refinement by Jana2006 on F^2	
Parameters refined, constraints, restraints	69, 4, 6
R_1, wR_2 (obs)	0.0218, 0.0508
R_1, wR_2 (all)	0.0277, 0.0527
GOF obs/all	1.47/1.40
$\Delta\rho_{min}$, $\Delta\rho_{max}$ (eÅ^{-3})	–0.70, 0.65
Weighting scheme, details	σ, $w = 1/(\sigma^2(I) + 0.0004I^2)$

Tab. 4 Atom positions, occupancies, and displacement parameters (in Å^2) for babánekite

	x/a	*y/b*	*z/c*	U_{eq}	U^{11}	U^{22}	U^{33}	U^{12}	U^{13}	U^{23}	*BV*
As	0.18474(4)	0	0.13164(7)	0.00955(11)	0.00547(17)	0.01346(19)	0.00880(17)	0	0.00029(12)	0	4.96(1)
Cu1#	0.5	0	0.5	0.01041(19)	0.0053(3)	0.0152(3)	0.0092(3)	0	–0.0006(2)	0	1.87(1)
Cu2#	0	0.11392(3)	0.5	0.01112(14)	0.0089(2)	0.0129(2)	0.0116(2)	0	0.00284(16)	0	1.90(1)
O1	0.3535(3)	0	0.1357(5)	0.0149(7)	0.0068(11)	0.0257(14)	0.0114(11)	0	0.0009(9)	0	1.86(1)
O2	0.15612(17)	0.10610(12)	0.2920(4)	0.0129(5)	0.0113(8)	0.0129(8)	0.0144(8)	0.0003(6)	0.0032(7)	–0.0027(7)	1.80(1)
O3	0.0978(2)	0	–0.2216(5)	0.0136(7)	0.0111(12)	0.0164(12)	0.0107(11)	0	–0.0018(9)	0	1.91(1)
O4	0.4019(2)	0.11629(16)	0.6978(4)	0.0251(7)	0.0113(90)	0.0418(13)	0.0192(10)	–0.0038(9)	–0.0014(7)	0.0077(9)	2.13(6)
O5	0.1012(2)	0.22550(14)	0.7839(4)	0.0215(6)	0.0236(10)	0.0209(10)	0.0203(9)	–0.0002(8)	0.0062(8)	–0.0008(8)	2.12(6)
H5a	0.044(3)	0.2831(15)	0.778(5)	0.0258*							1.02(5)
H4a	0.381(3)	0.097(2)	0.879(4)	0.0302*							1.01(5)
H5b	0.128(3)	0.2060(19)	0.990(3)	0.0258*							1.00(3)
H4b	0.3132(17)	0.126(2)	0.560(5)	0.0302*							1.05(3)

U_{eq} is defined as a third of the trace of the orthogonalized U^{ij} tensor
* – refined with isotropic displacement parameters. # – refined occupancies for Cu1 and Cu2 sites are 0.973(3) and 0.974(2), respectively
BV – bond-valence sums calculated using Dist option in Jana2006: bond-valence parameters taken from Gagné and Hawthorne (2015)

Regarding the fact that Co, Ni, Cu and Zn (confirmed by the microprobe analysis) have very similar scattering curves, only Cu was used in the later refinement as a proxy. Both the constrained and unconstrained refinement, which took into account the presence of all atoms mentioned above (and also allowing some degree of the ordering) in the cationic octahedral sites, did not lead either to better or more reasonable results. The constrained refinement fixing the composition, expressed by the empirical formula obtained from the electron-microprobe study, converged to the much worse indices of agreement (R = 0.0290, wR = 4.01, GOF = 2.41 for 864 unique observed reflections) compared to the fit using just the Cu at the sites. Positions of the hydrogen atoms were localized from difference-Fourier maps. The distance between the H atom and the corresponding donor O atom was constrained during the refinement (with a soft constraint of 0.90 Å with a certain weight, that produced *D*–H lengths in the range 0.74(3)–0.86(3) Å). The displacement parameters of the H atoms were set to be $1.2 \times U_{iso}$ of the corresponding donor O atom. The final cycles converged with R = 0.0218, wR = 0.0508 and GOF = 1.47 for 864 observed unique reflections. The correctness of the refined structure model was confirmed by an independent structure solution employing the charge-flipping method (Palatinus and Chapuis 2007). This independent solution obtained differs from the model based on Wildner et al. (1996) only in the order of the estimated errors. Atom positions, displacement parameters and results of the bond valence analysis are listed in Tabs 4 to 5. Some of the geometrical characteristics (also given in Tab. 4) were calculated using the program Vesta (Momma and Izumi 2008). The bond-valence analysis was carried out following the procedure of Brown (2002). The CIF file, also containing a block with the reflections, is deposited at the Journal's web page *www.jgeosci.org*.

5.1. Crystal structure

The refined structure of babánekite shows characteristic features of the vivianite-type minerals and synthetic compounds, characterized by the general formula $Me^{2+}_3(XO_4)_2 \cdot 8H_2O$ (*Me* = Mg, Fe, Co, Ni, Zn; *X* = P, As) (Mori and Ito 1950; Cesbron et al. 1977; Hill 1979; Fejdi et al. 1980; Giuseppetti and Tadini 1982; Dormann et al. 1982; Takagi et al. 1986; Riou et al. 1989; Bartl 1989; Wildner et al. 1996; Yakubovich et al. 2001; Capitelli et al. 2007, 2012; Assani et al. 2010; Yoshiasa et al. 2016; Antao and Dhaliwal 2017). Vivianite-type structures consist of $MeO_2(H_2O)_4$ octahedra and dimers of $Me2_2O_6(H_2O)_4$ octahedra that are linked via XO_4 tetrahedra (where *X* = P, As and probably can be also V) and hydrogen bonds to form complex layers parallel to (010). Adjacent layers are linked by hydrogen bonds only (Fig. 6).

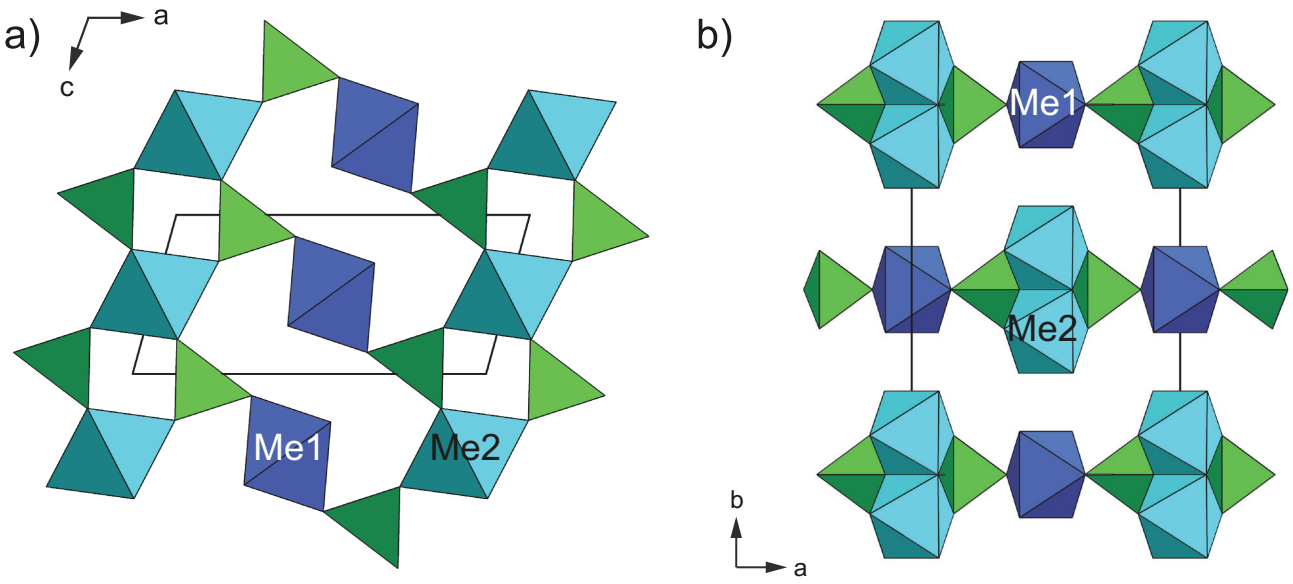

Fig. 6 The crystal structure of babánekite. **a** – Part of infinite sheet viewed along [010] consisting of vertex-sharing *Me1* and *Me2* distorted octahedra and AsO_4 tetrahedra (in green). **b** – The stacking of infinite sheets perpendicular to [010]; adjacent sheets are linked by H-bonds (H atoms and bonds omitted for clarity). Unit-cell edges are outlined in black solid lines.

The Me^{2+} cations, in babánekite dominantly Cu^{2+}, occupy two symmetrically distinct sites with the site-symmetries 2/*m* and 2 (Wyckoff sites 2*d* and 4*h* of the space group *C*2/*m*). The Cu1-centred (*Me*1) polyhedron forms a monomeric entity, which is linked *via* arsenate group to the dimer of Cu2-centred (*Me*2) polyhedra. The Cu1-centred polyhedron is considerably more irregular (in the terms of "effective coordination number", ECoN = 5.07, bond-length distortion index Δ = 0.05) than the Cu2-centred polyhedron (ECoN = 6.00, Δ = 0.003). This is a general feature also observed for other members of the vivianite-group of minerals (e.g., Giuseppetti and Tadini 1982, Yakubovich et al. 2001). It is probably caused due to less-firmly bonded ligands to the *Me*1 site: only two atoms are O^{2-} cations, the rest of the ligands represent the H_2O groups. The bonding in dimers of the *Me*2-centered polyhedra is much more rigid: only four of the ten ligands belong to the H_2O groups.

6. Discussion: the vivianite group of minerals – nomenclature issues

The present description of babánekite enlarges the family of As-dominant members in the vivianite group to seven. In Tab. 6, a general comparison of these members is given based on

Tab. 5 Selected interatomic distances (in Å) in the crystal structure of babánekite

Cu1–O1	1.961(2)	Cu2–O2	2.084(2)
Cu1–O1^{iv}	1.961(2)	Cu2–O2^{vi}	2.084(2)
Cu1–O4	2.201(2)	Cu2–O3^{vii}	2.099(1)
Cu1–O4^{iv}	2.201(2)	Cu2–O3^{viii}	2.099(1)
Cu1–O4^{v}	2.201(2)	Cu2–O5	2.101(2)
Cu1–O4^{i}	2.201(2)	Cu2–O5^{vi}	2.101(2)
<Cu1–O>	2.122	<Cu1–O>	2.094
V_P	12.59	V_P	12.19
σ^2	7.18	σ^2	6.95
Δ	0.051	Δ	0.003
ECoN	5.067	ECoN	5.998

As–O1	1.712(3)	
As–O2	1.684(2)	
As–O2^{i}	1.684(2)	
As–O3	1.676(2)	
<As1–O>	1.690	

H–bonds			
	D···H	*D*–A	<*D*–H···*A*>
O4–H4a···O1^{vii}	0.98(2)	2.753(3)	151(3)
O4–H4b···O2	0.973(16)	2.725(2)	164(3)
O5–H5a···O4^{xv}	0.97(2)	2.899(3)	167.7(18)
O5–H5b···O2^{vii}	0.982(14)	2.833(3)	151(2)

Δ, Bond-length distortion after Brown and Shannon (1973); σ^2, bond-angle distortion after Robinson et al. (1971); ECoN, effective coordination number after Hoppe (1979); V_P, polyhedral volume (in Å^3)
Calculations by Vesta (Momma and Izumi 2008)
Symmetry codes: (i) *x*, –*y*, *z*; (ii) *x*, *y*, *z*–1; (iii) *x*, 2*y*, *z*–1; (iv) –*x*+1, *y*, –*z*+1; (v) –*x*+1, –*y*, –*z*+1; (vi) –*x*, *y*, –*z*+1; (vii) *x*, *y*, *z*+1; (viii) –*x*, *y*, –*z*; (ix) –*x*, *y*, –*z*–1; (x) *x*+1/2, –*y*+1/2, *z*; (xi) –*x*+1/2, –*y*+1/2, –*z*+1; (xii) –*x*+1/2, –*y*+1/2, –*z*+2; (xiii) –*x*+1, *y*, –*z*+2; (xiv) –*x*, *y*, –*z*+2; (xv) *x*–1/2, –*y*+1/2, *z*

Tab. 6 Comparison of crystallographic and optical data for As-dominant members of vivianite group of minerals

mineral	**babánekite**	**erythrite**	**annabergite**	**hörnesite**	**manganohörnesite**	**köttigite**	**parasymplesite**
type locality	Jáchymov, CZ	Schneeberg, Germany	Annaberg, Germany	Banat, Hungary	Långban, Sweden	Schneeberg, Germany	Kiura Mine, Japan
reference	this paper	Wildner et al. (1996)	Wildner et al. (1996)	Palache et al. (1951)	Gabrielson (1954)	Dana (1850)	Ito et al. (1954)
Me^{2+} (ideal.)	Cu	Co	Ni	Mg	$(Mn^{2+}, Mg)_3$	Zn	Fe^{2+}
Me^{2+} (meas.)	$(Cu_{1.12}Zn_{0.78}Co_{0.69}Ni_{0.32})_{\Sigma 2.91}$	$(Co_{2.01}Fe_{0.74}Ni_{0.25})_{\Sigma 3.00}$	$(Ni_{2.48}Mg_{0.50}Fe_{0.02})_{\Sigma 3.00}$	–	$(Mn_{1.65}Mg_{1.32})_{\Sigma 2.97}$	$(Zn_{2.44}Co_{0.42}Ni_{0.14})_{\Sigma 3.00}$ [2]	–
space group	*C*2/*m*	*C*2/*m*	*C*2/*m*	*C*2/*m*	$P2_1/c$	*C*2/*m*	*C*2/*m*
a	10.1729(3)	10.251(3)	10.179(2)	10.137(2) [1]	10.38	10.241(3)	10.276(4) [2]
b	13.5088(4)	13.447(4)	13.309(3)	13.445(2)	28.09	13.405(3)	13.480(5)
c	4.7496(1)	4.764(1)	4.725(1)	4.754(1)	4.774	4.757(2)	4.771(2)
β	105.399(2)	104.98(1)	105.00(1)	101.73(2)	105.7	105.21(2)	105.02(5)
V	629.28(3)	634.4	618.2	634.17	1340.04	630.2(2)	–
Z	2	2	2	2	4	2	2
strongest lines	6.743/100	6.65/100 [#]	6.58/100 [#]	8.55/10 [#]	8.19 (80)	7.95 (37) [3]	7.91 (70)
in XRD	7.936/11	7.89/6	7.82/25	5.11/5	7.01 (100)	6.70 (100)	6.68 (100)
powder pattern	3.23/14	3.34/8	4.33/20	4.30/6	3.25 (60)	3.22 (39)	4.41 (40)
	2.715/11	3.22/12	3.18/26	3.59/9	3.09 (60)	2.99 (28)	3.91 (30)
	1.686/16	2.70/8	2.98/30	3.45/4	3.02 (70)	2.73 (26)	3.24 (50)
optical data		Biaxial (+) [#]	Biaxial (+) [#]	Biaxial (+) [#]	Biaxial (+) [#]	Biaxial (+)	Biaxial (+) [#]
		α = 1.622–1.629	α = 1.622	α = 1.563	α = 1.579	α = 1.619–1.622	α = 1.620–1.628
	N_{calc} = 1.662	β = 1.660–1.663	β = 1.658	β = 1.571	β = 1.589	β = 1.638–1.645	β = 1.648–1.660
		γ = 1.681–1.701	γ = 1.687	γ = 1.596	γ = 1.609	γ = 1.671–1.681	γ = 1.685–1.705
		2*V* = up to 90°	2*V* = 84°	2*V* = 65°	2*V* = 65–70°	2*V* = 74–85°	2*V* = 86°

[1] unit-cell parameters from Jambor and Dutrizac (1995)
[2] from Sturman (1976)
[3] calculated, Hill (1979)
[#] in Anthony et al. (1990)

the available data from the literature and the current study. For all these minerals, a broad cationic isomorphy is observed (Jambor and Dutrizac 1995, and others). The Me^{2+} cations occupy two symmetrically distinct sites in their crystal structure. On the one hand, partial ordering of cations at the *Me*1/*Me*2 sites was documented by the structure studies for some of the Mg-containing members of the vivianite group (Giuseppetti and Tadini 1982; Rojo et al. 1996; Wildner et al. 1996; Yakubovich et al. 2001). On the other hand, for the members containing Co, Zn, Ni or Cu (Hill 1979; Wildner et al. 1996; Capitelli et al. 2007; this study) no such a preference for a certain site was found. Theoretically this can be an artefact, caused by the problematic refinement due to the very similar scattering curves of Co, Ni, Cu and Zn, and therefore impossibility to discern them successfully using X-rays at the same site. Based on current study, the preference of Cu^{2+} for the Cu1 site, which is far more irregular than the Cu2 site (stronger effect of the Jahn-Teller distortion), even though highly probable, also cannot be reliably documented from current X-ray diffraction data. However, the possible preferential entering of the cations was discussed in the study of Antao and Dhaliwal (2017) who documented dominance of the heavier cations (Co, Ni, Zn) at *Me*1 site and lighter cations (Fe^{2+}) at the *Me*2 site. Nowadays, the classification of the particular mineral member of the vivianite group is based on the dominant cation at both sites (i.e. Σ(*Me*1+*Me*2): Sturman and Mandarino 1976; Giuseppetti and Tadini 1982; Yakubovich et al. 2001).

There have been several descriptions of the increased Cu^{2+} contents in mineral members of the vivianite group. A significant Cu^{2+} content in erythrite from Silberberg, near Rattenberg, Tyrol (Austria) was reported by Putz et al. (2012) and from Leogang, Salzburg by Auer (2017). Babánekite has been also found in Germany in the Clara mine (Blaß and Draxler 2015). Recently, we studied other samples from the Geister

vein, Jáchymov (Czech Republic) and also determined Cu-enriched köttigite (up to 0.99 Cu *pfu*), erythrite (up to 0.98 Cu *pfu*) and annabergite (up to 0.41 Cu *pfu*). The research on these mineral varieties is still ongoing and the results will be the subject of a forthcoming paper.

Acknowledgements. We thank Karla Fejfarová (BIOCEV, ASCR, v.v.i. and Charles University in Prague) and Michal Dušek (Institute of Physics, ASCR, v.v.i.) for help with analytical works. The manuscript benefited from thorough reviews of an anonymous reviewer and Uwe Kolitsch. Handling editor František Laufek is acknowledged for taking care of the manuscript. This research was supported by the project of GAČR No. 17-09161S to J.P. and J.S.

Electronic supplementary material. Supplementary crystallographic data for this paper (including the selected interatomic distances, results of bond-valence analysis and a CIF file) are available online at the Journal website *(http://dx.doi.org/10.3190/jgeosci. 248)*.

References

Antao SM, Dhaliwal I (2017) Growth oscillatory zoning in erythrite, ideally $Co_3(AsO_4)_2 \cdot 8H_2O$: Structural variations in vivianite-group minerals. Minerals 7: 136, DOI 10.3390/min7080136

Anthony JW, Bideaux RA, Bladh KW, Nichols MC (1990) Handbook of Mineralogy IV, Arsenates, Phosphates, Vanadates. Mineral Data Publishing, Tucson, Arizona, pp 1–680

Assani A, Saadi M, El Ammari L (2010) Dicobalt copper bis[orthophosphate(V)] monohydrate, $Co_{2.39}Cu_{0.61}(PO_4)_2 \cdot H_2O$. Acta Crystallogr E66: i44

Auer C (2017) 2035) Babanekit vom Nöckelberg bei Leogang, Salzburg. In: Walter F (ed) Neue Mineralfunde aus Österreich LXVI, Carinthia II, 207/127: 254–255 (in German)

Bartl H (1989) Water of crystallization and its hydrogen-bonded crosslinking in vivianite $Fe_3(PO_4)_2 \cdot 8H_2O$; a neutron diffraction investigation. Fresenius Zeit Anal Chem 333: 401–403

Blass G, Draxler V (2015) Babánekit, ein Erstfund für die Grube Clara im Schwarzwald. Mineralien-Welt 26: 16–19 (in German)

Brown ID (2002) The Chemical Bond in Inorganic Chemistry. The Bond Valence Model. Oxford University Press, Oxford, pp 1–278

Brown ID, Shannon RD (1973) Empirical bond-strength bond-length curves for oxides. Acta Crystallogr A29: 266–282

Burnham CW (1962) Lattice constant refinement. Carnegie Institute Washington Yearbook 61: 132–135

Capitelli F, Elaatmani M, Lalaoui MD, Piniella JF (2007) Crystal structure of a vivianite-type mineral: Mg-rich erythrite, $Co_{2.16}Ni_{0.24}Mg_{0.60})(AsO_4)_2 \cdot 8H_2O$. Z Kristallogr 222: 676–679

Capitelli F, Chita G, Ghiara MR, Rossi M (2012) Crystal-chemical investigation of $Fe_3(PO_4)_2 \cdot 8H_2O$ vivianite minerals. Z Kristallogr 227: 92–101

Cesbron F, Sichere MC, Vachey H (1977) Crystallographic properties and thermal behavior of compounds of the koettigite–parasymplesite series. Bull Soc franç Minéral Cristallog 100: 310–314 (in French)

Dana JD (1850) Köttigite. In: A System of Mineralogy, 3rd Edition. George P. Putnam, New York and London, pp 487

Dormann J-L, Gaspérin M, Poullen J-F (1982) Etude structurale de la sequence d'oxydation de la vivianite $Fe_3(PO_4)_2 \cdot 8H_2O$. Bull Minéral 105: 147–160

Fejdi P, Poullen J-F, Gaspérin M (1980) Affinement de la structure de la vivianite $Fe_3(PO_4)_2 \cdot 8H_2O$. Bull Soc franç Minéral Cristallogr 103: 135–138

Gabrielson O (1954) Manganiferous hoernesite and manganese-hoernesite from Långban, Sweden. Arkiv Mineral Geol 1: 333–337

Gagné OC, Hawthorne FC (2015) Comprehensive derivation of bond-valence parameters for ion pairs involving oxygen. Acta Cryst B71: 562–578

Giuseppetti G, Tadini C (1982) The crystal structure of cabrerite, $(Ni,Mg)_3(AsO_4)_2 \cdot 8H_2O$, a variety of annabergite. Bull Soc franç Minéral Cristallogr 105: 333–337

Haidinger W (1853) In: Vogl JF Drei neue Mineral-Vorkommen von Joachimsthal. Jb K-Kön Reichsanst 4: 221–223

Hill RJ (1979) The crystal structure of köttigite. Amer Miner 64: 376–382

Hloušek J, Plášil J, Sejkora J, Škácha P (2014) News and new minerals from Jáchymov, Czech Republic (2003–2014). Bull mineral-petrolog odd Nár Muz (Praha) 22: 155–181 (in Czech with English abstract)

Hoppe R (1979) Effective coordination number (ECoN) and mean-fictive ionic radii (Mefir). Z Kristallogr 150: 23–52

Ito T, Minato H, Sakurai K (1954) Parasymplesite, a new mineral polymorphous with symplesite. Proc Japan Acad 30: 318–324

Jambor JL, Dutrizac JE (1995) Solid solutions in annabergite–erythrite–hörnesite synthetic system. Canad Mineral 33: 1063–1071

Momma K, Izumi F (2008) *VESTA*: a three-dimensional visualization system for electronic and structural analysis. J Appl Cryst 41: 653–658

Mori H, Ito T (1950) The structure of vivianite and symplesite. Acta Cryst 3: 1–6

Ondruš P (1995) ZDS – software for analysis of X-ray powder diffraction patterns. Version 6.01. User's Guide. Prague, 1–120

Ondruš P, Veselovský F, Skála R, Císařová I, Hloušek J, Frýda J, Vavřín I, Čejka J, Gabašová A (1997) New naturally occurring phases of secondary origin from Jáchymov (Joachimsthal). J Czech Geol Soc 42: 77–108

Ondruš P, Veselovský F, Gabašová A, Hloušek J, Šrein V, Vavřín I, Skála R, Sejkora J, Drábek M (2003) Primary minerals of the Jáchymov ore district. J Czech Geol Soc 48: 19–147

Palache C, Berman H, Frondel C (1951) The System of Mineralogy of James Dwight Dana and Edward Salisbury Dana, Yale University 1837–1892, Volume II. Halides, Nitrates, Borates, Carbonates, Sulfates, Phosphates, Arsenates, Tungstates, Molybdates, etc. John Wiley & Sons, New York, pp 1–755

Palatinus L, Chapuis G (2007) Superflip – a computer program for the solution of crystal structures by charge flipping in arbitrary dimensions. J Appl Cryst 40: 451–456

Petříček V, Dušek M, Palatinus L (2014) Crystallographic Computing System JANA2006: general features. Z Krist 229: 345–352

Plášil J, Sejkora J, Škoda R, Novák M, Kasatkin AV, Škácha P, Veselovský F, Fejfarová K, Ondruš P (2014a) Hloušekite, (Ni,Co)$Cu_4(AsO_4)_2(AsO_3OH)_2(H_2O)_9$, a new member of the lindackerite supergroup from Jáchymov, Czech Republic. Mineral Mag 78: 1341–1353

Plášil J, Kasatkin AV, Škoda R, Škácha P (2014b) Klajite, $MnCu_4(AsO_4)_2(AsO_3OH)_2(H_2O)_{10}$, from Jáchymov (Czech Republic): the second world occurrence. Mineral Mag 78: 134–143

Pouchou JL, Pichoir F (1985) "*PAP*" (φρZ) procedure for improved quantitative microanalysis. In: Armstrong JT (ed) Microbeam Analysis. San Francisco Press, San Francisco, pp 104–106

Putz H, Lechner A, Poeverlein R (2012) Erythrin und Clarait vom Pichlerstollen am Silberberg bei Rattenberg, Nordtirol. Lapis 37: 47–52

Riou A, Cudennec Y, Gérault Y (1989) Cobalt(II) orthophosphate octahydrate. Acta Cryst C45: 1412–1413

Robinson K, Gibbs GV, Ribbe PH (1971) Quadratic elongation: a quantitative measure of distortion in coordination polyhedra. Science 172: 567–570

Rojo JM, Mesa JL, Pizarro JL, Lezama L, Arriortua MI, Rojo T (1996) Spectroscopic and magnetic study of the $(Mg,M)_3(AsO_4)_2{\cdot}8H_2O$ (M = Ni^{2+}, Co^{2+}) arsenates. Mater Res Bull 31: 925–934

Sejkora J, Ondruš P, Novák M (2010) Veselovskýite, triclinic $(Zn,Cu,Co)Cu_4(AsO_4)_2(AsO_3OH)_2{\cdot}9H_2O$, a Zn-dominant analogue of lindackerite. Neu Jb Mineral, Abh 187: 83–90

Sturman BD (1976) New data for köttigite and parasymplesite. Canad Mineral 14: 437–441

Sturman BD, Mandarino JA (1976) Barićite, the magnesium analogue of vivianite, from Yukon Territory, Canada. Canad Mineral 14: 403–406

Škácha P, Horák J, Plášil J (2014) Minerals and finds of ore shoots on the Geister vein of the western part of the Jáchymov ore district (Czech Republic). Bull mineralpetrolog odd Nár Muz (Praha) 22: 202–214

Takagi S, Mathew M, Brown WE (1986) Crystal structures of bobierrite and synthetic $Mg_3(PO_4)_2{\cdot}8H_2O$. Amer Miner 71: 1229–1233

Vogl JF (1854) Der neue Silbererz-Anbruch auf dem Geistergange zu Joachimsthal am 1. Oktober 1833. Jb K-Kön Reichsanst 5: 630–640

Vogl JF (1856a) Die sekundären Gebilde der Joachimsthaler Grube. Österr Z Berg- u Hüttenwes 45: 353–355

Vogl JF (1856b) Die sekundären Gebilde der Joachimsthaler Grube. Österr Z Berg u Hüttenwes 46: 361–362

Wildner M, Giester G, Lengauer CL, McCammon CA (1996) Structure and crystal chemistry of vivianite-type compounds: crystal structures of erythrite and annabergite with a Mössbauer study of erythrite. Eur J Mineral 8: 187–192

Yakubovich OV, Massa W, Liferovich RP, McCammon CA (2001) The crystal structure of barićite, $(Mg_{1.70}Fe_{1.30})(PO_4)_2{\cdot}8H_2O$, the magnesium-dominant member of the vivianite group. Canad Mineral 39: 1317–1324

Yoshiasa A, Miyano Y, Isobe H, Sugiyama K, Arima H, Nakatsuka A, Momma K, Miyawaki R (2016) Structural refinement of köttigite–parasymplesite solid solution: Unique cation site occupancy and chemical bonding with water molecules. J Mineral Petrolog Sci 111: 363–369